JOC Article

Quantum Chemical Calculations on the Peterson Olefination with α-Silyl Ester Enolates

Malcolm B. Gillies, Janne E. Tønder, David Tanner, and Per-Ola Norrby*

Department of Chemistry, Organic Chemistry, Technical University of Denmark, Building 201, Kemitorvet, DK-2800 Kgs. Lyngby, Denmark

pon@kemi.dtu.dk

Received July 18, 2002

The reaction of stabilized Peterson reagents (α-silyl ester enolates) with ketones has been studied theoretically and experimentally. Enolate geometry was studied by trapping experiments and NMR spectroscopy and was found to differ markedly with the nature of the base (LiHMDS vs LDA vs KHMDS). The chelating effect of the lithium counterion was found to be critical for the reaction. For the two ketones studied, the combined weight of experimental and computational data assigns geometrical selectivity to the initial addition transition state, though in general there appears to be a fine balance between three possible choices for the rate-determining step.

Introduction

Olefination reactions are important tools in organic synthesis, and since the pioneering work by Wittig,[1] a variety of reagents have been found for the conversion of carbonyl compounds to alkenes. In addition to phosphorus species,[2] there are important and widely used reagents based on sulfur (Julia reagents[3]) and silicon (Peterson reagents[4]) (Scheme 1). Factors influencing the selection of the appropriate olefination reagent[5] for a given application include chemo- and diastereoselectivity, reactivity, and accessibility. The Peterson reagents offer an interesting profile: their reactivity is high enough to allow reaction with both ketones and aldehydes; the reagents are frequently more *Z*-selective than the corresponding stabilized phosphorus reagents;[6] the silicon reagents are available via several synthetic routes.

The present investigation was prompted by earlier work on the application of olefination reactions in asymmetric synthesis.[7] In particular, the most efficient non-

SCHEME 1. Olefination Reactions

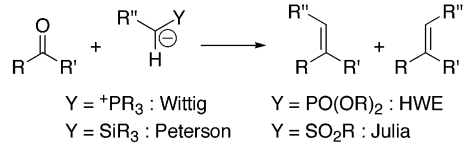

SCHEME 2. Diastereoconvergent Synthesis Employing Asymmetric HWE Reagents

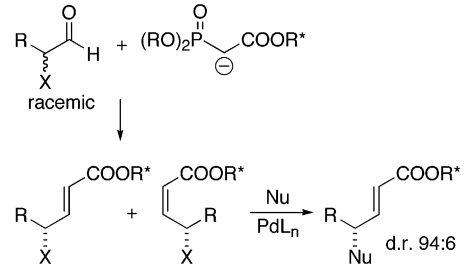

enzymatic diastereoconvergent protocol to date could be realized by combining the enantiodivergent[8] asymmetric Horner−Wadsworth−Emmons (HWE) reaction[9] with a stereospecific (*E*)-selective Pd-catalyzed allylic alkylation (Scheme 2), converting both enantiomers of a racemic aldehyde to one isomer of a γ-substituted α,β-unsaturated ester in high yield and diastereomeric purity without the need for separation of diastereomeric intermediates.[10]

In an attempt to widen the scope of the diastereoconvergent protocol, we have initiated an investigation of the closest silicon analogue of the HWE reaction, addition of α-silyl ester enolates (stabilized Peterson reagents) to carbonyl compounds. Here we report the first results of this study, a computational and experimental investiga-

* To whom correspondence should be addressed. Fax: (+45) 45933968.

(1) (a) Wittig, G.; Geissler, G. *Liebigs Ann. Chem.* **1953**, *580*, 44−57. (b) Wittig, G.; Schöllkopf, U. *Chem. Ber.* **1954**, *87*, 1318−1330.

(2) Maryanoff, B. E.; Reitz, A. B. *Chem. Rev.* **1989**, *89*, 863−927.

(3) (a) Julia, M.; Paris, J.-M. *Tetrahedron Lett.* **1973**, *14*, 4833−4836. For a review, see: (b) Kocienski, P. In *Comprehensive Organic Synthesis*; Trost, B. M., Fleming, I., Eds.; Pergamon Press: Oxford, 1991; Vol. 6, pp 987−1000. Recent development: (c) Baudin, J. B.; Hareau, G.; Julia, S. A.; Lorne, R.; Ruel, O. *Bull. Soc. Chim. Fr.* **1993**, *130*, 856−878.

(4) (a) Peterson, D. J. *J. Org. Chem.* **1968**, *33*, 780−784. For reviews, see: (b) Ager, D. J. *Org. React.* **1990**, *38*, 1−223. (c) Barrett, A. G. M.; Hill, J. M.; Wallace, E. M.; Flygare, J. A. *Synlett* **1991**, 764−770. (d) van Staden, L. F.; Gravestock, D.; Ager, D. J. *Chem. Soc. Rev.* **2002**, *31*, 195−200.

(5) For a comparison of olefination methods, see: Kelly, S. E. In *Comprehensive Organic Synthesis*; Trost, B. M., Fleming, I., Eds.; Pergamon Press: Oxford, 1991; Vol. 1, pp 730−817.

(6) (a) Larson, G. L.; Prieto, J. A.; Hernández, A. *Tetrahedron Lett.* **1981**, *22*, 1575−1578. (b) Kojima, S.; Inai, H.; Hidaka, T.; Ohkata, K. *Chem. Commun.* **2000**, 1795−1796.

(7) (a) Rein, T.; Pedersen, T. M. *Synthesis* **2002**, 579−594. (b) Rein, T.; Reiser, O. *Acta Chem. Scand.* **1996**, *50*, 369−379.

(8) Faber, K. *Chem. Eur. J.* **2001**, *7*, 5004−5010.

(9) Pedersen, T. M.; Jensen, J. F.; Humble, R. E.; Rein, T.; Tanner, D.; Bodmann, K.; Reiser, O. *Org. Lett.* **2000**, *2*, 535−538.

(10) Pedersen, T. M.; Hansen, E. L.; Kane, J.; Rein, T.; Helquist, P.; Norrby, P.-O.; Tanner, D. *J. Am. Chem. Soc.* **2001**, *123*, 9738−9742.

10.1021/jo0262107 CCC: $22.00
Published on Web 09/18/2002

SCHEME 3. Model Peterson Reaction

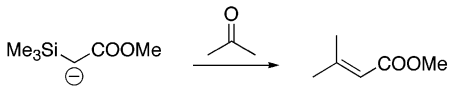

tion of the reaction path for a small model system, viz. the reaction between methyl trimethylsilyl acetate and acetone (Scheme 3). Characterization of the rate- and selectivity-determining steps and the influence of the enolate counterion have been of particular interest. We have also compared the results with the previously published study of the closely related HWE reaction.[11,12] The goal of the current work was to increase our understanding of the selectivity-determining step(s) in the synthetically very useful Peterson reaction, for which there is a surprising lack of theoretical studies. The Wittig reaction and other phosphorus-based olefinations have been subjected to several theoretical investigations,[11−13] but as far as we are aware, for the Peterson reaction previous computational work has been limited to CNDO calculations.[14] In future experimental work, an appropriate chiral auxiliary will be used, and chiral, racemic ketones will be investigated as substrates, in close analogy to previously published HWE developments.[7,9−12,15] To the best of our knowledge, there is but a single example in the literature of a chiral ester being used as an auxiliary in an asymmetric Peterson olefination reaction.[16] In preparation for future studies of the asymmetric version of this reaction, we have here investigated the reaction between the model Peterson reagent and a simple, chiral ketone, 2-methyl cyclohexanone.

Computational Methods

Scheme 4 shows the proposed mechanism for the Peterson reaction with all relevant intermediates, based on the closely related HWE reaction.[11] The enolate starting material may be one of two diastereomers, cis and trans,[17] resulting in two convergent reaction pathways. The geometries of these ground-state structures, together with the intervening transition states were optimized using density functional calculations with the B3LYP hybrid functional[18] and the 6-31G* basis set, with

SCHEME 4. Proposed Mechanism for the Peterson Reaction (counterion omitted). Pre- and Post-Complexes (3a/3b and 6) Are Not Shown

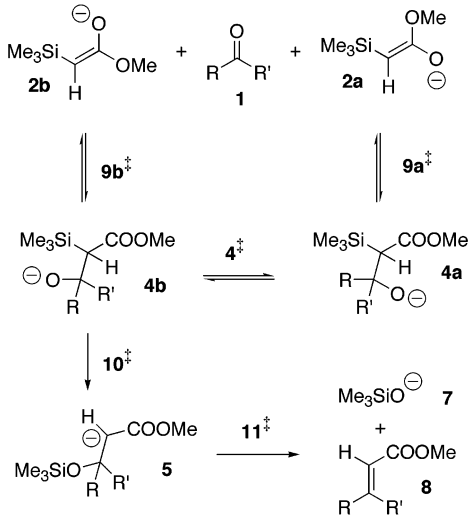

acetone as starting material **1**. Single point energies of selected stationary points were calculated with various sized basis sets (6-31G*, 6-311+G**, 6-311+G(2df,2p)) at the MP2 correlated level. Geometry optimizations at the B3LYP/6-31G* level were also carried out for transition states **9a‡**, **9b‡**, **4‡**, and **10‡** of the reaction with 2-methylcyclohexanone as starting material **1**. All stationary points on the acetone reaction PES were optimized using the polarizable continuum Poisson−Boltzmann solvation model available in Jaguar,[19] while single point solvation energies were calculated for the remaining gas-phase structures. We also determined gas-phase stationary points and single-point solvation energies for the acetone system with explicit coordination of two THF molecules to lithium for **9a‡**, **9b‡**, and **10‡**. Cartesian coordinates for all optimized structures are provided as Supporting Information.

The pseudospectral Jaguar program (version 4.1)[20] was used for all B3LYP calculations, and Gaussian 98 (revision A.11.3)[21] was used for all MP2 calculations. The solvent parameters were a dielectric coefficient of 7.43 and a probe radius of 252 pm, appropriate for THF; cavity and surface area terms were not included in the solvation calculations. The solution-phase calculations used settings for "ultra-fine" SCF accuracy and "fine" DFT grids

(11) (a) Brandt, P.; Norrby, P.-O.; Martin, I.; Rein, T. *J. Org. Chem.* **1998**, *63*, 1280−1289. (b) Rein, T.; Vares, L.; Kawasaki, I.; Pedersen, T. M.; Norrby, P.-O.; Brandt, P.; Tanner, D. *Phosphorus, Sulfur Silicon* **1999**, *144−146*, 169−172.

(12) Norrby, P.-O.; Brandt, P.; Rein, T. *J. Org. Chem.* **1999**, *64*, 5845−5852.

(13) For recent examples, see: (a) Lu, W. C.; Wong, N. B.; Zhang, R. Q. *Theor. Chem. Acc.* **2002**, *107*, 206−210. (b) Yamataka, H.; Nagase, S. *J. Am. Chem. Soc.* **1998**, *120*, 7530−7536. (c) Armstrong, D. R.; Barr, D.; Davidson, M. G.; Hutton, G.; O'Brien, P.; Snaith, R.; Warren, S. *J. Organomet. Chem.* **1997**, *529*, 29−33.

(14) Trindle, C.; Hwang, J.-T.; Carey, F. A. *J. Org. Chem.* **1973**, *38*, 8, 2664−2669.

(15) For leading references, see: (a) Mendlik, M. T.; Cottard, M.; Rein, T.; Helquist, P. *Tetrahedron Lett.* **1997**, *38*, 6375−6378. (b) Kreuder, R.; Rein, T.; Reiser, O. *Tetrahedron Lett.* **1997**, *38*, 9035−9038. (c) Tullis, J. S.; Helquist, P.; Rein, T. *Phosphorus, Sulfur Silicon* **1999**, *144−146*, 165−168. (d) Vares, L.; Rein, T. *Org. Lett.* **2000**, *2*, 2611−2614.

(16) Gais, H.-J.; Schmiedl, G.; Ossenkamp, R. K. L. *Liebigs Ann./Recueil* **1997**, 2419−2431.

(17) To avoid confusion resulting from counterion dependent priority in the *E*/*Z*-nomenclature for enolates, cis and trans refer to the relationship between silyl and the enolate oxygen. Thus, the cis enolate **2b** corresponds to (*E*)-enolate with Li^+ or no counterion, the (*Z*)-enolate with K^+, and gives the (*Z*)-enol ether on silyl trapping.

(18) (a) Becke, A. D. *J. Chem. Phys.* **1993**, *98*, 5648−5652. (b) Lee, C.; Yang, W.; Parr, R. G. *Phys. Rev. B* **1988**, *37*, 785−789.

(19) Marten, B.; Kim, K.; Cortis, C.; Friesner, R. A.; Murphy, R. B.; Ringnalda, M. N.; Sitkoff, D.; Honig, B. *J. Phys. Chem.* **1996**, *100*, 11775−11788.

(20) http://www.schrodinger.com.

(21) Frisch, M. J.; Trucks, G. W.; Schlegel, H. B.; Scuseria, G. E.; Robb, M. A.; Cheeseman, J. R.; Zakrzewski, V. G.; Montgomery, J. A., Jr.; Stratmann, R. E.; Burant, J. C.; Dapprich, S.; Millam, J. M.; Daniels, A. D.; Kudin, K. N.; Strain, M. C.; Farkas, O.; Tomasi, J.; Barone, V.; Cossi, M.; Cammi, R.; Mennucci, B.; Pomelli, C.; Adamo, C.; Clifford, S.; Ochterski, J.; Petersson, G. A.; Ayala, P. Y.; Cui, Q.; Morokuma, K.; Salvador, P.; Dannenberg, J. J.; Malick, D. K.; Rabuck, A. D.; Raghavachari, K.; Foresman, J. B.; Cioslowski, J.; Ortiz, J. V.; Baboul, A. G.; Stefanov, B. B.; Liu, G.; Liashenko, A.; Piskorz, P.; Komaromi, I.; Gomperts, R.; Martin, R. L.; Fox, D. J.; Keith, T.; Al-Laham, M. A.; Peng, C. Y.; Nanayakkara, A.; Challacombe, M.; Gill, P. M. W.; Johnson, B.; Chen, W.; Wong, M. W.; Andres, J. L.; Gonzalez, C.; Head-Gordon, M.; Replogle, E. S.; Pople, J. A. Gaussian, Inc., Pittsburgh, PA, 2001.

TABLE 1. Energies of the Stationary Points along the Reaction Path from Acetone

	energy relative to lowest pre-reactive state kJ mol^{-1}			
	Li			no Li
	ΔG^a	ΔE^b	ΔE_{SPC}	ΔE^b
1 + 2a	0	29.3	29.2	6.0
1 + 2b	19.5	44.6	52.9	4.6
3a	6.0	0	0	2.8
3b	20.4	11.5	4.8	0
9a‡	40.8	20.2	3.3	48
9b‡	54.5	33.4	24.6	47.5
4a	18.5	−10.1	−23.4	38.5
4‡	33.9	4.2	−9.1	–
4b	12.8	−14.3	−29.1	38.2
10‡	62.7	33.2	21.9	39.9
5	−19.1	−41.4	−54.4	−45.4
11‡	−7.1	−27.8	−43.3	−35.8
6	−109.5	−122.8	−132.2	−97.8
7 + 8	−140.1	−117.5	−127.8	−107.1

[a] Obtained from ΔE by addition of ZPE and ΔG_{vib} calculated at the corresponding gas-phase geometry. [b] Optimized in solvent, including contributions from solvation but not from vibration. [c] Energy in solvent, calculated at the gas-phase geometry.

(see Supporting Information for Jaguar input file examples). Whenever possible, all solution-phase stationary points were also optimized in the gas phase and validated as either minima or saddle points by analysis of the analytical frequencies. Gas-phase DFT calculations were performed with "accurate" SCF accuracy and "medium" grid density.

Transition state optimizations were started from geometries derived from scans along the expected bond-making/breaking reaction coordinates, with the analytical gas-phase Hessians used initially. Transition states in solvent were confirmed by the presence of a single negative frequency in the updated Hessian.[22] We performed normal-mode analysis of all stationary points on the gas-phase PES to give zero point energies and vibrational free energy correction terms at the temperature of the typical reaction conditions, 200 K. Energies were calculated without scaling of the Hessian.[23] For stationary points that could be located in both solvent and gas phase, and that showed strong similarity between the two structures,[24] the ZPE and free energy contributions from the gas-phase calculation were applied to the corresponding solvated stationary point to yield a final, composite free energy.

Results

Energies for all stationary points along the reaction path with acetone as substrate, with and without coordinating Li^+ counterion, can be found in Table 1. Paths from trans and cis reagent are denoted **a** and **b**, respectively.[17] Note that at intermediate **4**, the paths converge via rotation TS **4**‡. As a validation for the combination of vibrational contributions from gas-phase geometries with solution-phase structures, Table 1 includes the corresponding solution phase energies calculated at the gas-phase geometries, and Table 2 demonstrates the small structural deviation between gas-phase and solution-structures for Li-coordinated species. Table 3 contains the results of MP2 single point energy calculations on a number of the B3LYP gas-phase stationary point geometries, with various sizes of basis set.

TABLE 2. Superimposed Geometries (all atoms excluding Li) for Corresponding Gas- and Solution-Phase Lithium-Coordinated Acetone Reaction Paths

	displacement (pm)							
	9a‡	**9b‡**	**4a**	**4‡**	**4b**	**10‡**	**5**	**11‡**
rms	6	14	3	5	11	7	6	15
maximum	15	24	7	11	20	13	12	26
lithium	12	84	21	16	32	31	33	21

TABLE 3. Single Point MP2 Energies for Selected Stationary Points from the Lithium-Coordinated Gas-Phase Acetone Reaction Path

	energy relative to **3a** (kJ mol^{-1})		
basis set	**3a**	**9a‡**	**10‡**
6-31G*	0	13.6	−23.4
6-311+G**	0	8.3	−13.2
6-311+G(2df,2p)	0	3.2	−31.8

TABLE 4. Energies of Selected Stationary Points along the Reaction Path from 2-Methylcyclohexanone

		energy (ΔG^a) kJ mol^{-1}			
configuration	product	**9a‡**	**9b‡**	**4‡**	**10‡**
RRR-eq	(*Z*)	27.8	36.6	–[b]	51.3
RRR-ax	(*Z*)	33.6	32.9	9.9	34.6
RRS-eq	(*E*)	37.2	39.3	37.2	46.2
RRS-ax	(*E*)	24.3	36.4	36.9	37.4
RSR-eq	(*E*)	9.1	33.1	13.7	53.8
RSR-ax	(*E*)	29.7	27.3	29.4	29.4
RSS-eq	(*Z*)	4.3	28.8	0	56.0
RSS-ax	(*Z*)	28.7	27.9	–[b]	36.5

[a] Energy in solvent, calculated at the gas-phase geometry, with addition of ZPE and ΔG_{vib}. [b] Converged geometries for these transition states could not be found.

Calculations on the reaction with 2-methylcyclohexanone as starting material are summarized in Table 4. Two new chiral centers are formed in the initial TS in addition to the center present in **1**, necessitating the investigation of four diastereomeric paths. Furthermore, two low-energy chair conformations are accessible to the cyclohexane moiety. We postulate that exchange between the two chair conformations is feasible, but that crossover between diastereomeric paths requires reversion to the starting materials. Thus, we must consider eight paths with pairwise crossover between conformers. We define the (*R*) stereoisomer of the starting material as the canonical configuration and list the stereocenter formed in the ketone and enolate fragments afterward.

The reactivities of enolates with two different counterions were tested in reactions with acetone (Scheme 3) and with cyclohexanone. Under otherwise identical conditions, the enolate derived from LHMDS and methyl trimethylsilyl acetate (**2**) gave good yields of unsaturated ester product **8** (96% in the case of methylcyclohexylideneacetate),[25] whereas the KHMDS-derived enolate

(22) Analytical second derivatives are not available for solvated systems in the Jaguar program, and accurate numerical frequency calculations are computationally intractable for this size of system, so we did not make this extra check of the transition states in solvent.

(23) Scott, A. P.; Radom, L. *J. Phys. Chem.* **1996**, *100*, 16502−16513.

(24) In the current work, we adhere to the following arbitrary similarity criteria: all-atom overlay rms deviation excluding Li: <15 pm; energy from full optimization in solvent lower than single point solvation at the gas-phase geometry, but not by more than 20 kJ mol^{-1}.

showed very low reactivity: no product could be detected in the reaction with acetone, while in the reaction with cyclohexanone only a 3% yield could be detected by GC-MS analysis (the major product, 61%, was instead the enol ether, 1-trimethylsilyloxycyclohexene).

Discussion

Use of Composite Free Energies. For all calculations involving the coordinating lithium cation (i.e., overall neutral systems), the geometries determined in the gas phase and solvent correspond surprisingly well. Thus, our best estimate of the total free energy in solution (G) is obtained as a composite, by adding the vibrational contributions calculated in the gas phase to the energies of the corresponding stationary points obtained with the solvation model. For verification, we also calculated the total free energy surface based on the more conventional method of adding all contributions calculated as single points for the gas-phase geometries. The relative energies on these two surfaces differ by no more than a few kJ mol^{-1} (the difference is the same as that between ΔE and ΔE_{SP} in Table 1).

For the anionic systems which have been used as a model, for the case with a weakly coordinating counterion like potassium[11] or lithium-12-crown-4, a proper gas-phase PES could not be obtained. Most stationary points on the PES are dependent on some type of stabilization of localized anionic charge, either by solvent or a coordinating counterion. In the absence of both these stabilizing factors, the low-energy path along the reaction coordinate displays a monotonic energy decrease, as has been observed previously for other ionic reactions in the gas phase.[26] We must therefore neglect the vibrational contributions for this reaction.[22] All energy comparisons including anionic structures are therefore performed at the highest accessible level, potential energy in solvent with added free energy solvent corrections, E (Table 1).

The calculations on the lithium-coordinated system in the absence of solvent gave stationary point geometries essentially identical to the solvated ones. All-atom superpositions of the corresponding stationary point structures have an rms deviation of 15 pm or less, excluding lithium in all cases (Table 2); the position of the coordinating lithium is slightly more variable. The relative energies of the stationary points are similar between the gas phase and solvated calculations, with the exception of the additional stabilization of intermediate **4** in the solvated case. The single-point solution-phase energies for the gas-phase minimum geometries present a picture that corresponds closely to the PES from the solution-phase minima. As expected, relaxation in solvent results in lower energies, the absolute energy differences between the two solution-phase energy curves being shown in Figure 1 (for clarity, only trans enolate pathway data points are shown). The average difference in energies is 7 kJ mol^{-1}, and the maximum is 18 kJ mol^{-1}, with the two curves close to parallel. These results support the use of single-point solvation energies where full relaxation is impractical, such as in the case of the 2-methylcyclohexanone reaction studied here.

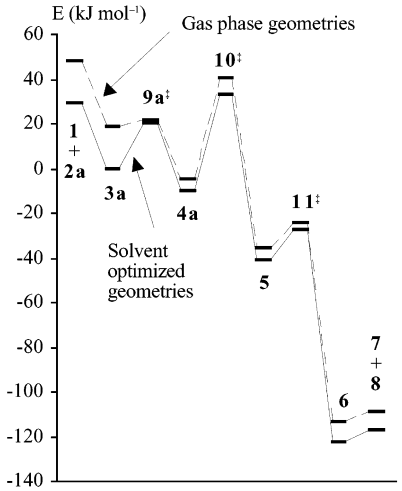

FIGURE 1. Absolute energy difference between single-point and fully relaxed solution potential energy surfaces (acetone reaction).

The close correspondence between the two systems gives additional confidence in the reliability of the solvated results and also provides the opportunity to make a prediction of a realistic free energy surface. Normal mode calculations on the gas-phase system give corrections for zero point energy, and vibrational enthalpy and entropy, based on a harmonic approximation. These corrections should be reasonable for the corresponding solvated structures.

Accuracy of Relative Free Energies. The accuracy of the calculated composite free energies is subject to a number of qualifications. The adequacy of the chosen basis set, the treatment of electron correlation, and the solvent model are matters for careful consideration. In particular, transition state **10‡**, which contains a pentavalent silicon, may be treated inaccurately by relatively low level calculations. The results in Table 3 showing the relative energy of transition states **9a‡** and **10‡** with larger basis sets and treatment of correlation at the MP2 level indicate that this energy difference is not captured well at the B3LYP/6-31G* level. The highest level calculation with a 6-311+G(2df,2p) basis set gave a gas-phase energy for **9a‡** 35 kJ mol^{-1} higher than **10‡**, whereas B3LYP/6-31G* gave a difference of only 2 kJ mol^{-1}. The resulting $\Delta\Delta E$ can be applied to the difference in composite free energy values to give a more realistic picture of the identity of the rate-determining step.

The implicit solvation model does not give a complete and accurate treatment of the effects of the coordination of solvent molecules to the solute. This may be an important omission in the case of the lithium counterion. A more realistic treatment of solvation would be to include an explicit solvation shell around Li. Such calculations are very demanding, but we succeeded in locating the TS **9‡** in the presence of two explicitly coordinating THF molecules. Encouragingly, the geometry of the TS is only marginally affected by the explicit solvation, except for the position of the lithium itself in the case of **9b‡**. In the presence of explicit solvation, the TS is in the expected six-membered ring chair of a regular

(25) Shimoji, K.; Taguchi, H.; Oshima, K.; Yamamoto, H.; Nozaki, H. *J. Am. Chem. Soc.* **1974**, *96*, 1620−1621.
(26) Hagelin, H.; Åkermark, B.; Norrby, P.-O. *Chem. Eur. J.* **1999**, *5*, 902−909.

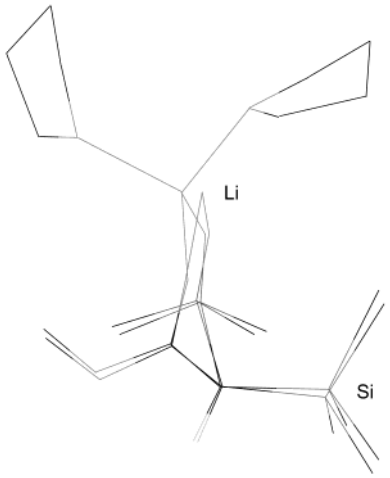

FIGURE 2. Superimposition of TS **9b‡** structures calculated with implicit THF solvation and with explicit coordination of two THF molecules to lithium.

aldol addition. Without the solvent shell, Li^+ is attracted to the electron density in the rest of the molecule, in particular to the slightly negative silyl-bonded methyls, giving a boatlike TS. The superimposition of the two structures can be seen in Figure 2. Since the O−Li−O moiety has no substituents in this model, there are none of the usual negative effects of a boat conformation like eclipsing or diaxial interactions. However, the proximity of the Li cation to the organic moiety causes an artifactual lowering of the total energy, composed partially of electrostatic attraction and partially of basis set deficiency effects. We can expect this error to cancel to a large extent when comparing very similar structures, like conformations, but to lower the predictivity when comparing structurally different complexes where the local environment around lithium changes.

Role of the Counterion. Most published procedures for Peterson reactions of α-silyl enolates employ lithium bases,[4] and it has previously been observed that potassium enolates are substantially less reactive than the corresponding lithium enolates.[27] We have verified that this difference in reactivity also exists in our model system. As mentioned previously, the potassium salt of methyl trimethylsilyl acetate did not yield any observable product with acetone and only 3% GC yield with cyclohexanone. Similar results were obtained when the lithium enolate was reacted in the presence of a slight excess of 12-crown-4 to disrupt the coordinating ability of lithium.[28] In contrast, under otherwise identical conditions, the lithium enolate reacted rapidly with both ketones, giving a 96% yield in the reaction with cyclohexanone. These results agree well with the computational study. In line with previous studies on the HWE reaction,[11] the free enolate anion was used as a model for the system with noncoordinating counterion. The most important points on the reaction profiles are depicted in Figure 3. In the absence of a coordinating metal, the approach of the ketone to the Peterson reagent can occur with either anti or one of two gauche relationships between silicon and ketone oxygen. Only results for the energetically most favored gauche structures for **9‡** and **4** are reproduced here.

SCHEME 5. Enolate Trapping Experiments

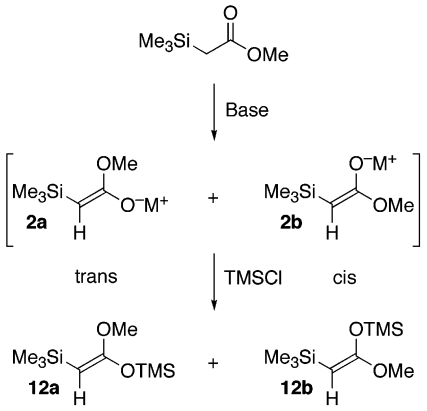

The difference in size of the initial activation barrier between the coordinated and noncoordinated cases amounts to 26 (26) kJ mol^{-1} (trans/cis) relative to the precomplex when calculated in solution, without vibrational corrections. In addition to the high initial activation energy, the noncoordinated reaction pathway differs in the absence of a stationary point for the rotation between **4a** and **4b**, and the intermediate dissociates rather than passing this barrier. The additional stabilization of intermediate **4** by Li^+ is evident on comparison of the calculated PES data, lying 47 (64) kJ mol^{-1} (**4a**/**4b**) lower relative to the precomplex **3**, and 21 (38) kJ mol^{-1} lower relative to transition state **9**, when Li coordination is present.

The much higher barrier in the absence of lithium provides a rationalization for the lack of reactivity observed in reactions between enolates of alkyl trialkylsilyl acetates and ketones under conditions lacking strongly coordinating counterions. Only activated ketones such as 2,3-epoxycyclohexanone have been reported to react when poorly coordinating counterions are present, the lack of reactivity of nonactivated ketones being ascribed to increased ketone enolization.[27] The same trend was also observed here: the O-silylated enol ether was the major product from reaction of cyclohexanone with the potassium salt of enolate **2**. Suppression of ketone enolization and the presence of a strongly coordinating cation thus appear to be vital for efficient Peterson olefination.[29]

Configuration of Enolate. The selectivity in the Peterson reaction is dependent on the configuration of the starting enolate, **2**. This has sometimes been assumed to be cis in the literature,[16] but our calculations indicate that the trans form is substantially more stable. To elucidate this critical point, we performed trapping experiments to determine the favored form and the configurational stability of the lithium enolate.

The Li enolates produced under varying conditions and one example of a K enolate were trapped by O-silylation using trimethylsilyl chloride (Scheme 5). The products

(27) Strekowski, L.; Visnick, M.; Battiste, M. A. *Tetrahedron Lett.* **1984**, *25*, 5603−5606.
(28) Tønder, J. E., unpublished results.
(29) For the use of cerium as counterion to circumvent enolization, see: Johnson, C. R.; Tait, B. D. *J. Org. Chem.* **1987**, *52*, 281−283. See also ref. 4d.

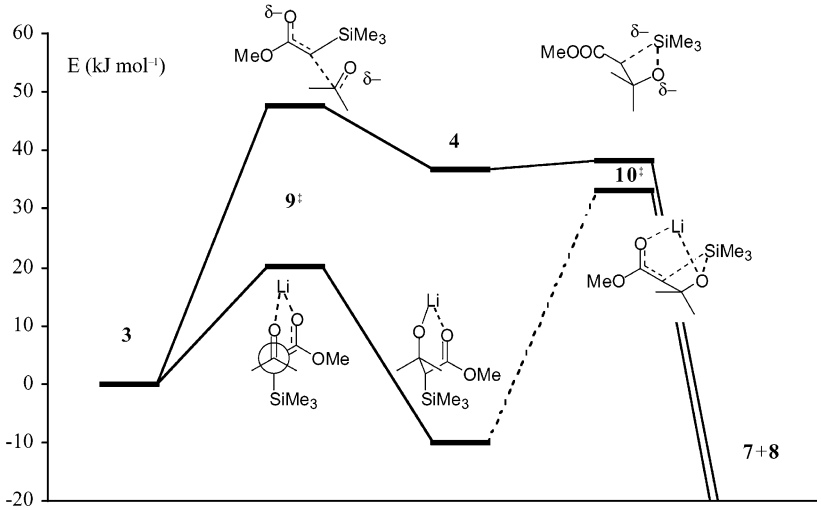

FIGURE 3. Reaction profiles with and without lithium counterion (reaction with acetone). Solution phase energies (ΔE) relative to precomplex **3**. Only the pathway proceeding from the trans enolate **3a** is shown. Gas-phase calculations failed to find any stationary points for the free anionic system. The absence of both the stabilizing effect of solvent and of a coordinating lithium gives a markedly different reaction pathway, and it appears that the entire pathway is downhill under these conditions.

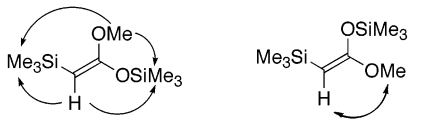

12a: weak NOE, <2% **12b**: strong NOE, >5%

FIGURE 4. NOE results for **12a** and **12b**.

TABLE 5. Enolate-Trapping Experiment. Results Are Based on ^{1}H NMR

experiment	base	temperature (°C)	**12a**:**12b**	yield (%)
1	LDA	−78	75:25	88
2	LDA	0	88:12	69
3	LiHMDS	−78	100:00	>99
4	LiHMDS	0	100:00	94
5	KHMDS	0	25:75	40

12 were assigned by 1D NOE experiments (Figure 4). The ratios of **12a**:**12b** are listed in Table 5.

The trans enolate **2a** turned out to be favored in all cases when lithium was used as counterion, sometimes being formed exclusively (Table 5). Furthermore, unequal ratios could be obtained even when the enolate was formed at 0 °C (entries 2 and 4, Table 5), giving strong indication that the enolate is configurationally stable under the trapping conditions at −78 °C.

In agreement with the literature,[30] the experiments with LDA as base show that the trans ratio increases when the enolate is formed at 0 °C, indicating that **2a** is the thermodynamically favored product, in good agreement with the computational results. The mixture obtained at −78 °C indicates that LDA is kinetically undiscriminating. On the other hand, LiHMDS gives exclusively trans enolate **2a** independent of reaction temperature. Interestingly enough, the potassium base favors the cis enolate **12b**. In line with the currently held view of kinetic deprotonation of nonsilylated esters,[31] it is probable that LiHMDS acts as a slow base, leaving some nondeprotonated ester in solution long enough for the ester and ester enolate to equilibrate in an identity reaction, giving the thermodynamically favored product exclusively. This type of equilibration could also be expected in the reaction mixture with an enolizable ketone substrate, which could rationalize the observation that enolates derived from LDA and LiHMDS give similar product selectivities[28] despite the differences in enolate ratio from these two bases.

Acetone Olefination Free Energy Surface with Li$^+$. The lithium-coordinated solution-phase reaction profile proceeding from acetone, including the vibrational free energy correction, is shown in Figure 5, along with the structures of the various stationary points. The coordination of the ketone and ester oxygens to the lithium ion largely predetermines the geometry of the reacting species in this case. The presence of the lithium ion also has a stabilizing effect on the various anionic species, particularly the oxyanion intermediate **4** where the negative charge is largely localized to the oxygen.

For both the gas-phase and the solvated Li-coordinated systems the calculated difference in energy between transition states **9b**‡ and **10**‡ at B3LYP/6-31G* is considerably smaller than the expected uncertainty in relative energies of 10 kJ mol^{-1}. Addition of the vibrational correction terms increases the free energy of **10**‡ by approximately 10 kJ mol^{-1} relative to **9b**‡, in line with expectation for the more conformationally restricted cyclic **10**‡; the transition state **9a**‡ lies lower, 22 kJ mol^{-1} below **10**‡. The rotational barrier between **4a** and **4b** is 29 kJ mol^{-1} lower than **10**‡. If we apply a correction from the MP2/6-311G+(2df,2p) results, **10**‡ is lowered significantly in energy relative to **9a**‡. Including solvation and vibration terms, this gives a free energy for **9a**‡ 11 kJ mol^{-1} above **10**‡. Thus, different theoretical levels give different predictions for the rate-determining step (RDS). We can estimate from the identified sources of error that a safe identification of the RDS would require at least

(30) Matsuda, I.; Murata, S.; Izumi, Y. *J. Org. Chem.* **1980**, *45*, 237−240.

(31) Ireland, R. E.; Daub, J. P. *J. Org. Chem.* **1981**, *46*, 479−485. For a review see Evans, D. A.; Nelson, J. V.; Taber, T. R. *Topics Stereochem.* **1982**, *13*, 1−115.

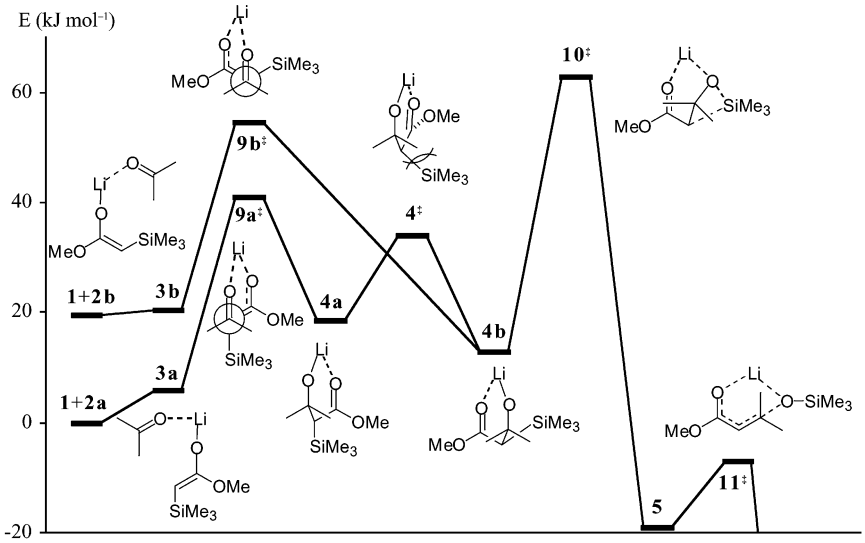

FIGURE 5. Free energy reaction profile (reaction with acetone).

explicit solvation on lithium, continuum solvation of the full complex, and correlation treatment beyond MP2 with at least a triple-ζ basis set. Including all these factors in one calculation is well beyond our current computational resources. Instead, it is possible to identify the RDS by a comparison with the very similar HWE reaction, where the selectivity is also determined in transition states very similar to **9‡** and **10‡**.[12] For the HWE, it was shown that the two transition states were very similar in energy, but with a very different sensitivity to steric crowding and solvation. Thus, with sterically demanding reactants, the ring closure/elimination TS (corresponding to **10‡**) was found to be rate determining, whereas for sterically unencumbered reactions, the RDS was the addition (**9‡**).[11] It has also been shown that addition of a mixed HWE/Peterson reagent, which can choose elimination toward phosphorus or silicon after the common addition step, exclusively followed the Peterson elimination route for all silyl groups smaller than triisopropylsilyl (TIPS).[32] This clearly shows that the elimination activation barrier is lower for silicon than for phosphorus. In conjunction with what is known about the relative energy of the addition and elimination steps for the HWE reaction, the result gives a strong indication that **9‡** is higher in energy than **10‡**, in agreement with the MP2 but not with the B3LYP/6-31G* energies.

Precomplex. The solvated potential energy *E* of the complex **3** between the anionic methyl TMS-acetate, lithium, and acetone is substantially lower than that of the separated starting materials **1** + **2**, one of the major reasons why the lithium ion lowers the barrier to addition. However, on the free energy surface, the precomplex is slightly higher in energy than the reactants, due mainly to the entropic penalty.

Transition State 9. Transition state **9a‡**, which leads to formation of a new C−C bond, is shown in Figure 6. We note that the addition is strongly reminiscent of a classical aldol addition. It has been observed that the isolated reagent in vacuo prefers a four-membered ring

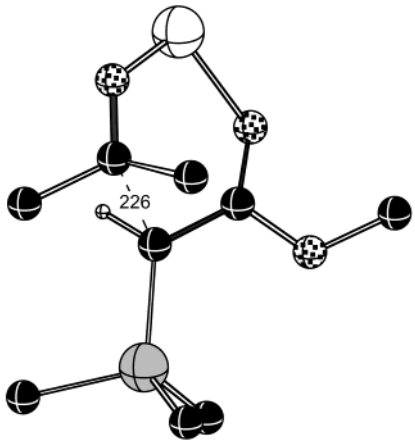

FIGURE 6. Transition state **9a‡**. Most hydrogen atoms have been omitted for clarity. Carbon atoms are shown in black, silicon in gray, and lithium and hydrogen in white. Oxygen is stippled. Bond lengths labeled in pm. The remaining structures follow the same conventions.

coordination of lithium,[13c] which has led to the proposal of the so-called "butterfly" transition state for the Peterson reaction.[32] However, as already noted by Warren and co-workers for the corresponding Horner−Wittig reaction,[13c] there is no Li−C coordination in the TS; even in the gas phase, the addition proceeds via a six-membered chairlike TS. The transition state is early, with a C−C distance of 226 (239) pm (**9a‡**/**9b‡**) in the solvated system. The gas-phase geometries are essentially identical to the solvated structures. The activation barrier is 10 (13) kJ mol^{-1} lower in the presence of solvent. The solvated transition state is somewhat later in the absence of lithium, with a C−C distance of 204 (203) pm (**9a‡**/**9b‡**), and a substantially higher activation barrier as expected from the Hammond postulate.[33] The trend in activation barriers, increasing in energy when either the coordinating lithium or the continuum solvation is removed, can be understood from the Bell−Evans−Polanyi principle.[33]

(32) Waschbüsch, R.; Carran, J.; Savignac, P. *Tetrahedron* **1996**, *52*, 14199−14216.

(33) Jensen, F. *Introduction to Computational Chemistry*; Wiley: Chichester, 1999.

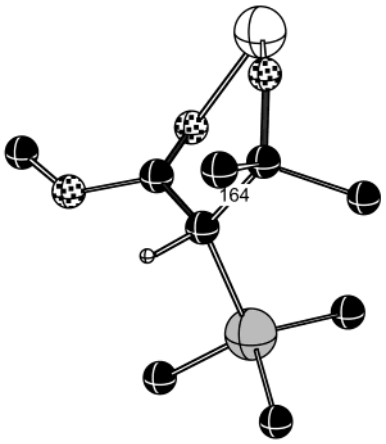

FIGURE 7. Transition state **4**‡.

The reaction leads from a conjugated enolate anion, with a fair gas-phase stability, to a localized oxyanion. Stabilization of the latter by either coordination to a cation or by continuum solvation will lower the energy of **4** relative to **3**, and thus lower the barrier to reaction from **3** to **4**.

Steric interactions in **9**‡ are determined by interaction between the ketone substituents and either the silyl or the ester moiety. In **9a**‡, both substituents are gauche to the silyl, but one is also crowded by being gauche to the ester. The larger substituent can therefore be expected to prefer the position anti to the ester moiety. Elimination via **10**‡ requires a 180 °C−C bond rotation, which would eclipse the larger substituent with the ester moiety. We should therefore expect *Z* selectivity from a rate-determining **9a**‡. In **9b**‡, both the silyl and the ester are gauche to one substituent and anti to the other. It is also possible for the TS to accommodate steric bulk by slight rotation. It is therefore difficult to make a general prediction for the selectivity in this TS. We will return to a specific example later.

Oxyanion Intermediate 4. Oxyanion intermediate **4** is computationally stable in both gas and solution phase for the coordinated system. Without lithium, only the solvated system was found to be a stationary point, in line with the previous finding that the HWE oxyanion intermediate was a nonstationary point at the B3LYP/6-31G* level.[11] The C−C bond is long, 163 (161) pm (**4a**/**4b**) for the solvated Li-coordinated intermediate, similar to the equivalent weak bond found for the HWE oxyanion intermediate.[11] In a Curtin−Hammett situation,[34] the relative energies of **4a** and **4b** have no influence on the observed selectivities. Intermediate **4b** is set up for direct elimination via **10**‡, whereas **4a** must first convert to **4b** via TS **4**‡.

Torsional Transition State 4. Torsional transition state **4**‡ is a simple torsional barrier between rotamers **4a** and **4b** (Figure 7), complicated by the coordination of two oxygens to the lithium. The reaction eigenvector includes a component of the lithium movement on a very soft PES. This poses unexpected problems, both in locating the TS for more substituted systems (vide infra) and for evaluating the free energy components. In addition, TS **4**‡ contains no partial bonds and is therefore expected to be well described by relatively low level of theory B3LYP. Transition states **9**‡ and **10**‡, on the other hand, do contain partial bonds and could therefore be expected to be lowered in energy relative to **4**‡ by inclusion of larger basis sets and/or higher correlation. The current results indicate that **4**‡ will not influence the reaction selectivity (as opposed to the related reaction of sulfur ylids with aldehydes[35]), but it cannot be excluded, and a final verdict will have to await higher level treatment or evaluation based on the selectivity profile. To this end, we note that the pro-(*E*) ketone substituent is eclipsed with the TMS group, with a C−Si distance of 325 pm. Thus, even at the currently calculated energy level, **4**‡ could be expected to function as a filter, prohibiting formation of (*E*)-product from trans-enolate **1a**.

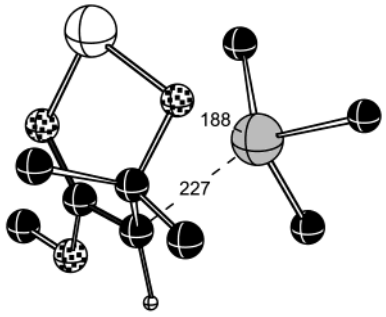

FIGURE 8. Transition state **10**.

Transition State 10. Cyclic transition state **10**‡ involves the concerted breaking of the Si−C bond together with the formation of a Si−O bond (Figure 8). The transition state is relatively late, with the Si−C bond weak at 227 pm for the solvated geometry. As with the HWE reaction, the ring geometry is quite puckered,[11] and the $C_{ester}-C-C-C_{pro-(Z)}$ dihedral makes an angle of 44°. TS **10**‡ includes two partial bonds, partial hypervalency at Si, variable coordination at Li, and also some close lithium−methyl interactions. We expect it to be the most difficult point on the PES to describe computationally. We can see that the energy of this TS relative to that of TS **9**‡ is very sensitive both to level of theory and to basis set. At B3LYP/6-31G*, including both solvation and vibration contributions to the free energy, TS **10**‡ seems to be rate determining. However, TS **10**‡ should yield overall (*E*)-selectivity due to the close proximity between the ester moiety and the pro-(*Z*) substituent, something that is rarely seen in the Peterson reaction. Furthermore, the MP2/6-311+G(2df,2p) correction lowers the energy of TS **10**‡ selectively. Thus, considering all sources of error in the calculations and comparing to experimental results, we would not expect TS **10**‡ to influence the selectivity of reagents with the simple TMS substituent. However, the picture is known to be different when bulkier silyl substituents are employed,[32] and like the related HWE reaction, might also be influenced by the choice of solvent.[11]

Enolate Intermediate 5 and Transition State 11. Formation of the enolate intermediate **5** is more exothermic than the preceding steps along the reaction path, and

(34) Maskill, H. *The Physical Basis of Organic Chemistry*; Oxford University Press: Oxford; 1985.

(35) Aggarwal, V. K.; Harvey, J. N.; Richardson, J. *J. Am. Chem. Soc.* **2002**, *124*, 5747−5756.

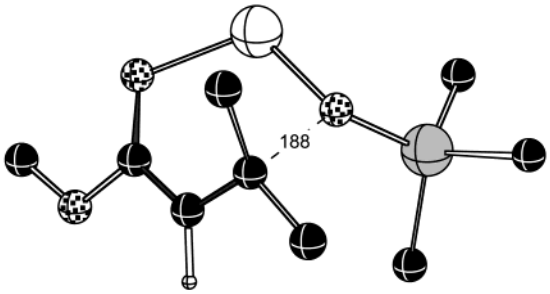

FIGURE 9. Transition state **11**‡.

the subsequent barrier to transition state **11**‡ is relatively low. The O−C bond to the TMS group is weak at 152 pm, as previously seen for the corresponding step in the HWE reaction.[11] The lifetime of the intermediate is likely to be short, making the likelihood of isomerization and potential loss of steric control due to C−C bond rotation fairly low. The transition state **11**‡ for the final elimination of TMSO anion is shown in Figure 9. The subsequent formation of the products is highly exothermic.

Origins of Selectivity. The Peterson reaction frequently displays a high *Z* selectivity, even with moderately encumbered ketones.[27] To rationalize this selectivity, we must find the points on the free energy surface where the pro-(*E*) ketone substituent is selectively crowded. First of all, we can see that the final TS **11**‡ is very product like, with crowding only of the pro-(*Z*) substituent. In any case where *Z*-selectivity is observed, TS **11**‡ cannot have an influence on the selectivity, and thus elimination through **11**‡ must be substantially faster than the competing bond rotation.

Product formation from **2a** is achieved through three additional transition states, **9a**‡, **4**‡, and **10**‡. For the parent system, the rate- and selectivity-determining barrier is **9a**‡, by a margin of 13 kJ mol^{-1} if the difference between MP2/6-311G+(2df,2p) single point energies is added as a correction to the free energies calculated at the solvated B3LYP/6-31G* level. As was demonstrated for the HWE reaction,[12] when the reaction must pass through a sequence of transition states with similar activation energies, each TS will act as a filter, blocking one or a few isomeric pathways while allowing others to form product. A high observed selectivity might then be the result of several transition states acting in concert. The same type of serial selectivity has also recently been demonstrated for the Aggarwal catalytic epoxidation of aldehydes,[35] where for the first time a torsional barrier like **4**‡ was found to affect the selectivity. In our case, **4**‡ is completely eclipsed and therefore expected to disfavor bulky groups in the pro-(*E*) substituent strongly and selectively due to crowding with the silyl group. In TS **10**‡, the strain is somewhat relieved, but the pro-(*E*) substituent is still crowded by the silyl group. However, the pro-(*Z*) substituent is now in closer proximity to the ester moiety, decreasing the selectivity of **10**‡ compared to **4**‡. In the initial addition, TS **9a**‡, the two substituents are staggered around the silyl group, but the pro-(*E*) substituent experiences additional crowding from the ester moiety. This could rationalize the earlier observation that (*Z*)-selectivity increases with the size of the ester moiety.[36] Thus, all three transition states would be expected to disfavor (*E*)-product. In contrast, TS **9b**‡ should yield low (if any) selectivity, since one substituent will be crowded by the silyl, and the other by the ester moiety. However, TS **9b**‡ is unlikely to influence the selectivity, since the preferred form of the reactant is **2a**, and equilibration of **2a** and **2b** can occur via reversible protonation involving the substrate.

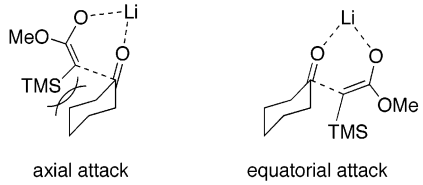

FIGURE 10. Axial and equatorial additions to cyclohexanone, **9a**‡.

2-Methylcyclohexanone Olefination Reaction Pathways. To elucidate the nature of the rate-determining step, we have investigated the reaction of reagent **2** with 2-methylcyclohexanone in detail. At −78 °C, this reaction gives a (*Z*):(*E*) ratio of 93:7 (slightly higher than the ratio of 89:11 found earlier[27]), corresponding to a barrier difference of 4.2 kJ mol^{-1}. We expect to be able to predict relative energies of similar transition states with high confidence, but as has been already shown, we cannot access a level of theory that will allow us to determine the relative energies of different transition states accurately enough. The enolate reagent has been shown to be formed in trans configuration when LiHMDS is used as base. We must therefore consider the sequence **9a**‡ → **4**‡ → **10**‡. We must also allow for the possibility of reversion of **4b** to cis enolate in situ via **9b**‡. If such reversion is feasible, readdition via other diastereomers of **9b**‡ must also be considered.

Four diastereomeric pathways are possible, depending on the face selectivity of both enolate and ketone in the initial addition, and the 2-methyl substituent may be axial or equatorial in each. Given that the reagent is nonchiral in this model, we have investigated only the (*R*)-enantiomer of the substrate. The enantiomeric form of each stationary point, derived from the (*S*)-enantiomer of the substrate, must have the same energy and result in the same diastereomer of the product. The diastereomeric transition states and intermediates will be designated by the configuration of each chiral center (e.g., *RRR*), where the first label corresponds to the 2-position in 2-methylcyclohexanone (always *R*), the second is the configuration of the former carbonyl carbon, and the third is the enolate α-position. The *RRR* and *RSS* diastereomers will lead to (*Z*) product, whereas *RRS* and *RSR* will lead to (*E*). Two chair forms with similar energies are possible, with the methyl group in either axial or equatorial position (labeled ax or eq, respectively).

We will first investigate the initial addition, **9a**‡. Somewhat unexpectedly for attack at a cyclohexanone, there is a very strong preference for equatorial attack. The TS is strongly oriented by the lithium, leading to severe repulsion between the cyclohexanone ring and the TMS group in any axial attack (Figure 10). We also see that for equatorial attack the axial 2-positions of the cyclohexanone are in close proximity to the TMS group.

(36) Larcheveque, M.; Legueut, C.; Debal, A.; Lallemand, J. Y. *Tetrahedron Lett.* **1981**, *22*, 1595−1598.

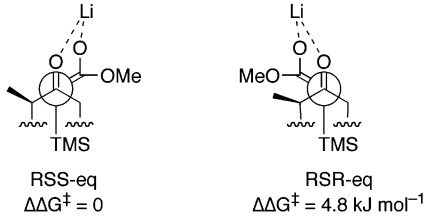

FIGURE 11. The two favored forms of **9a**‡.

The energy penalty even for methyl substitution in these positions is severe, much more so than for a mere axial cyclohexane substituent.

All in all, only two of the eight possible addition modes are energetically feasible, *RSS*-eq and *RSR*-eq (Figure 11). All other isomers of **9a**‡ are at least 20 kJ mol^{-1} higher than these two. The pro-(*E*) isomer, *RSR*-eq, is higher in energy by 4.8 kJ mol^{-1}, corresponding very well to the experimental (*Z*)-preference.

Transition state **4**‡ is in many ways similar to **9a**‡. Interaction energies are higher, due to the shorter interatomic distances and the fact that substituents are now eclipsed. The absolute calculated barriers at our highest accessible level usually differ by only a few kJ mol^{-1} from the corresponding isomers of **9a**‡. However, comparing the two favored isomers from **9a**‡, the energy difference in **4**‡ has been increased to 13.7 kJ mol^{-1}, in poor agreement with the experimental results. We therefore consider it unlikely that **4**‡ influences the selectivity, and that the high calculated energies are artifactual. A likely source for the error is the application of a harmonic approximation in the evaluation of the vibrational contributions to the free energies of this floppy TS.

At this point, we will briefly consider TS **9b**‡. In agreement with the BEP principle,[33] the TS leading to the high energy cis enolate **2b** is generally higher in energy than the TS to **2a** and always more than 20 kJ mol^{-1} higher than the most favored form of **9a**‡, RSS-eq. Formation of cis enolate in situ by the addition−reversion route can therefore be excluded in this system.

Looking finally at TS **10**‡, the calculated energies of this TS are substantially higher than those for TS **9a**‡. However, we have identified several reasons why this high energy may be an artifact. Looking at the selectivity profile expected from TS **10**‡, we see that the major difference between the isomeric forms lies in the interactions of the methyl substituent. As stated for the acetone model, all pro-(*Z*) forms will show an interaction between the substituent and the ester moiety, whereas the substituent only interacts with the enolate hydrogen in the pro-(*E*) forms. Interestingly, the methyl group prefers an axial conformation for all diastereomers. *RSR* is lowest in energy, with pro-(*Z*) forms *RRR* and *RSS* disfavored by 5.3 and 6.9 kJ mol^{-1}, respectively. A rate-determining TS **10**‡ is therefore at odds with the experimental picture.

Returning to the most likely RDS, **9a**‡, we wish to point out that the existing chiral center has a strong influence on the configuration of the former carbonyl carbon (Felkin−Anh−Eisenstein-type selectivity), whereas the enolate α-carbon is only weakly affected. The former preference is > 20 kJ mol^{-1}, whereas the latter is ca. 4 kJ mol^{-1}. Both of these conditions are necessary for a successful application of our recently introduced enantioconvergent protocol.[10] It is very important for the correct selectivity that the carbonyl is strongly affected by the existing chiral center, but that the enolate is not, allowing for introduction of chiral auxiliaries in the Peterson reagent.

Finally, as a note of caution, we wish to point out that although the B3LYP/6-31G* level employed here is very popular in mechanistic investigations, it is clear from the present results that, for anionic systems, errors of at least 30 kJ mol^{-1} can be expected in the comparison of electronically dissimilar transition states, even when accounting for solvent effects. We would thus like to stress the necessity of careful validation, preferably by comparison of selected computational predictions with experimental data.

Conclusions

The preferred configuration of lithium enolates of simple α-silyl esters is trans, **2a**.[17] The reaction of this enolate with a ketone proceeds through four transition states, three of which can act as a selective filters and prohibit selective paths, in analogy with the previously investigated HWE reaction[11,12] and Aggarwal's aldehyde epoxidation.[35] At least two of these transition states are expected to disfavor (*E*)-product. The final elimination of lithium siloxide is expected to be facile, and faster than bond rotation and stereochemical scrambling in **5**. *Z* selectivity in the addition of 2-methylcyclohexanone appears to be determined by the initial transition state **9a**‡, and the predicted product ratio is in good accordance with experiment. The mechanistic insight provided by the present study is currently being exploited for design of stereoselective Peterson reagents suitable for asymmetric synthesis. Results will be reported in due course.

Experimental Section

General. Tetrahydrofuran was distilled under nitrogen from sodium/benzophenone prior to use. All reactions were carried out in oven-dried glassware and under nitrogen. Commercially available compounds were used as received.

Peterson Reactions with LiHMDS. Acetone. LiHMDS (1.0 M in THF, 1.40 mL, 1.4 mmol) was added over a period of 2 min to a solution of methyl trimethylsilyl acetate (0.25 mL, 1.4 mmol) in THF (6 mL) at 0 °C. The resulting yellow solution was stirred for 30 min at 0 °C. The temperature was then lowered to −78 °C, and acetone (0.11 mL, 1.5 mmol) was added dropwise to the reaction mixture. Stirring was continued at −78 °C for 2 h. Saturated ammonium chloride (10 mL) was added, and the mixture was extracted with diethyl ether. GC-MS of this extract showed the desired product (methyl 3,3-dimethylacrylate) and hexamethyldisilazane. No attempt was made to isolate the product due to its high volatility. Both methyl 3,3-dimethylacrylate[37] and hexamethyldisilazane[38] showed MS data in accord with those previously reported.

Cyclohexanone. LiHMDS (1.0 M in THF, 1.40 mL, 1.4 mmol) was added over a period of 2 min to a solution of methyl trimethylsilyl acetate (0.25 mL, 1.4 mmol) in THF (6 mL) at 0 °C. The resulting yellow solution was stirred for 30 min at 0 °C. The temperature was then lowered to −78 °C, and cyclohexanone (0.16 mL, 1.5 mmol) was added dropwise to the reaction mixture. Stirring was continued at −78 °C for 2 h.

(37) Leung-Toung, R.; Wentrup, C. *Tetrahedron* **1992**, *48*, 7641−7654.
(38) Sharkey, A. G., Jr.; Friedel, R. A.; Langer, S. H. *Anal. Chem.* **1957**, *29*, 770−776.

Saturated ammonium chloride (10 mL) was added, and the mixture was extracted with diethyl ether. GC-MS of this extract showed that 96% of the cyclohexanone had been converted into the desired product (methyl cyclohexylideneacetate) and that 4% unreacted cyclohexanone was left. The combined organic extracts were dried ($MgSO_4$), and the solvent was evaporated to give 0.208 g (96%) of methyl cyclohexylideneacetate with ^{1}H NMR and MS spectral data in accord with those reported earlier.[39,40] The crude product was >95% pure, according to ^{1}H NMR.

2-Methylcyclohexanone. LiHMDS (1.0 M in THF, 1.40 mL, 1.4 mmol) was added to a 0 °C solution of methyl trimethylsilyl acetate (0.25 mL, 1.5 mmol) in THF (3 mL). The resulting yellow solution was stirred for 30 min at 0 °C, before the temperature was lowered to −78 °C. 2-Methyl cyclohexanone (0.18 mL, 1.5 mmol) was added dropwise, and stirring continued at −78 °C for 2 h. Ammonium chloride (sat. solution, 10 mL) was added, and the mixture was extracted with diethyl ether, dried ($MgSO_4$), and evaporated to give 164 mg of a colorless oil. ^{1}H NMR showed a mixture of the (*Z*)- and (*E*)-isomer in a relationship of 92:8. Gas chromatography showed a (*Z*/*E*) relationship of 93:7. Separation of the two isomers by column chromatography was not possible.

The ^{1}H NMR data of the (*Z*)-isomer were in accordance with those reported earlier.[41] It was not possible to assign all signals from the (*E*)-isomer as most of them were overlapped by the signals from the (*Z*)-isomer. HRMS *m*/*z* calcd for $C_{10}H_{16}O_2$ (M^+) 168.1150, found 168.1156.

Attempted Peterson Reactions with KHMDS. Acetone. KHMDS (279 mg, 1.5 mmol) was added to a solution of methyl trimethylsilyl acetate (0.25 mL, 1.4 mmol) in THF (6 mL) at 0 °C. The resulting yellow solution was stirred for 30 min at 0 °C. The temperature was then lowered to −78 °C, and acetone (0.11 mL, 1.5 mmol) was added dropwise. Stirring was continued at −78 °C for 2 h. Saturated ammonium chloride (10 mL) was added, and the mixture was extracted with diethyl ether. GC-MS of this extract showed only hexamethyldisilazane.[38]

Cyclohexanone. KHMDS (279 mg, 1.5 mmol) was added to a solution of methyl trimethylsilyl acetate (0.25 mL, 1.4 mmol) in THF (6 mL) at 0 °C. The resulting yellow solution was stirred for 30 min at 0 °C. The temperature was then lowered to −78 °C, and cyclohexanone (0.16 mL, 1.5 mmol) was added dropwise. Stirring was continued at −78 °C for 2 h. Saturated ammonium chloride (10 mL) was added, and the mixture was extracted with diethyl ether. GC-MS of this extract showed that only 3% of the desired product (methyl cyclohexylideneacetate) had formed, whereas 36% cyclohexanone was left unchanged and 61% 1-trimethylsilyloxycyclohexene had formed. The MS data for methyl cyclohexylideneacetate[40] and 1-trimethylsilyloxycyclohexene[42] were in accord with those described earlier. No attempt was made to isolate the products.

Enolate-Trapping Experiments. LiHMDS, −78 °C. LiHMDS (1.0 M in THF, 1.5 mL, 1.5 mmol) was added to a −78 °C solution of methyl trimethylsilyl acetate (0.25 mL, 1.5 mmol) in THF (6 mL). The resulting yellow solution was stirred for 60 min at −78 °C. TMSCl (0.29 mL, 2.25 mmol) was then added dropwise. Stirring was continued at −78 °C for 2 h before application of vacuum (2.5 mmHg) for removal of the THF. $CDCl_3$ was added to the solid residue and the suspension filtered through cotton into an NMR tube. ^{1}H NMR showed only one species, which was assigned as the trans-isomer **12a** by means of 1D differential NOE (Figure 4). The ^{1}H and ^{13}C NMR data are listed in Table 6.

TABLE 6. 300 MHz NMR Data ($CDCl_3$) for 12a and 12b (ppm)

^{1}H NMR	OCH_3	CH	$OSi(CH_3)_3$	$Si(CH_3)_3$
12a	3.49	3.08	0.26	0.03
12b	3.54	2.97	0.20	0.05
^{13}C NMR	CO_2	OCH_3	CH	$OSi(CH_3)_3$
12a	161.59	72.78	54.00	0.17
12b	164.67	63.94	55.05	0.49

LiHMDS, 0 °C. LiHMDS (1.0 M in THF, 1.5 mL, 1.5 mmol) was added to a 0 °C solution of methyl trimethylsilyl acetate (0.25 mL, 1.5 mmol) in THF (6 mL). The resulting yellow solution was stirred for 30 min at 0 °C. TMSCl (0.29 mL, 2.25 mmol) was then added dropwise. Stirring was continued at 0 °C for 1 h before application of vacuum (2.5 mmHg) for removal of the THF. $CDCl_3$ was added to the solid residue and the suspension filtered through cotton into an NMR tube. Apart from 6% unconverted starting material, ^{1}H NMR showed only the trans isomer **12a**.

LDA, −78 °C. Butyllithium (1.6 M in hexanes, 0.94 mL, 1.5 mmol) was added to a 0 °C solution of diisopropylamine (0.21 mL, 1.5 mmol) in THF (6 mL), and stirring was continued for 30 min. The solution was cooled to −78 °C, whereupon methyl trimethylsilyl acetate (0.25 mL, 1.5 mmol) was slowly added. The resulting yellow solution was stirred for 60 min at −78 °C. TMSCl (0.29 mL, 2.25 mmol) was then added dropwise. Stirring was continued at −78 °C for 2 h before application of vacuum (2.5 mmHg) for removal of the THF. $CDCl_3$ was added to the solid residue and the suspension filtered through cotton into an NMR tube. In addition to 12% unconverted starting material, ^{1}H NMR showed the two isomers (**12a** and **12b**) in a 75:25 relationship (see Table 5 and Table 6).

LDA, 0 °C. Butyllithium (1.6 M in hexanes, 0.94 mL, 1.5 mmol) was added to a 0 °C solution of diisopropylamine (0.21 mL, 1.5 mmol) in THF (6 mL), and stirring was continued for 30 min. Methyl trimethylsilyl acetate (0.25 mL, 1.5 mmol) was slowly added and the solution stirred for 30 min at 0 °C. TMSCl (0.29 mL, 2.25 mmol) was then added dropwise and stirring was continued at 0 °C for 1 h, before application of vacuum (2.5 mmHg) for removal of the THF. $CDCl_3$ was added to the solid residue and the suspension filtered through cotton into an NMR tube. In addition to 31% unconverted starting material, ^{1}H NMR showed the two isomers (**12a** and **12b**) in a 88:12 relationship (see Table 5 and Table 6).

KHMDS. KHMDS (299 mg, 1.5 mmol) was added to a 0 °C solution of methyl trimethylsilyl acetate (0.25 mL, 1.5 mmol) in THF (6 mL). The resulting mixture was stirred for 30 min at 0 °C. TMSCl (0.29 mL, 2.25 mmol) was then added dropwise. Stirring was continued at 0 °C for 1 h before application of vacuum (2.5 mmHg) and removal of the THF. $CDCl_3$ was added to the residue and the suspension filtered through cotton into an NMR tube. In addition to 60% unconverted starting material, ^{1}H NMR showed the two isomers (**12a** and **12b**) in a 25:75 relationship (see Table 5 and Table 6).

Acknowledgment. Financial support from the Danish Natural Sciences Research Council, the Carlsberg Foundation, the Lundbeck Foundation, and the Torkil Holm Foundation is gratefully acknowledged. J.E.T. thanks Novo Nordisk for support. We thank Professor Tobias Rein for stimulating discussions.

Supporting Information Available: Examples of Jaguar input files. Cartesian coordinates and raw energies of computationally characterized species (ASCII). This material is available free of charge via the Internet at http://pubs.acs.org.

JO0262107

(39) Hamdouchi, C.; Topolski, M.; Goedken, V.; Walborsky, H. M. *J. Org. Chem.* **1993**, *58*, 3148−3155.
(40) Hon, Y.-S.; Lu, L. *Tetrahedron* **1995**, *51*, 7937−7942.
(41) Duraisamy, M.; Walborsky, H. M. *J. Am. Chem. Soc.* **1983**, *105*, 3252−3264.
(42) Hydrio, J.; Van de Weghe, P.; Collin, J. *Synthesis* **1997**, *1*, 68−72.